

## Supporting Information

for *Adv. Mater. Interfaces*, DOI: 10.1002/admi.202101291

Near-Infrared Multilayer MoS<sub>2</sub> Photoconductivity-  
Enabled Ultrasensitive Homogeneous Plasmonic  
Colorimetric Biosensing

*Younggeun Park,\* Byunghoon Ryu, Seung Jun Ki,  
Xiaogan Liang,\* and Katsuo Kurabayashi\**

## Supporting Information

**Near-infrared Multilayer MoS<sub>2</sub> photoconductivity-Enabled Ultrasensitive Homogeneous Plasmonic Colorimetric Biosensing**

*Younggeun Park\**, *Byunghoon Ry*, *Seung Jun Ki*, *Xiaogan Liang\**, and *Katsuo Kurabayashi\**

**List of contents****METHODS**

**Table 1. Detection performances of commercialized human CEA ELISA kits.**

**Supplementary Figures**

**Fig. S1. Micro-printing-based MoS<sub>2</sub> pattern fabrication.**

**Fig. S2. Time-domain root-mean-square (RMS) noise values of MoS<sub>2</sub> photoconducting channels.**

**Fig. S3. AFM (a) images and (b) thickness profiles of MoS<sub>2</sub> layers i) 2.5, ii) 7.5, iii) 12.5, and 25 nm.**

**Fig. S4. Multilayer MoS<sub>2</sub> channel photocurrent as a function of illumination power.**

**Fig. S5. Fabrication steps of multilayer MoS<sub>2</sub> channel-integrated colorimetric reader device.**

**Fig. S6. *I-V* curves of multilayer MoS<sub>2</sub> channel-integrated colorimetric reader device loaded with PBS, WB, and Urine with excitation illumination at (a)  $\lambda = 530$  nm and (b)  $\lambda = 650$  nm.**

**Fig. S7. *I-V* curves of multilayer MoS<sub>2</sub> channel-integrated colorimetric reader device for various CEA concentrations with excitation illumination (a)  $\lambda = 530$  nm and (b)  $\lambda = 650$  nm.**

**References**

**METHODS**

**Chemicals:** We purchased gold nanoparticle (gold nanosphere (AuNPs,  $d = 50\text{nm}$ ) from Tedpella, 10-Carboxy-1-decanethiol (C-10) and Albumin from bovine serum (BSA) from Sigma Aldrich, 1-ethyl-3-[3-dimethylaminopropyl] carbodiimide (EDC) and/ N-hydroxysuccinimide (NHS) from Thermo Co., respectively. We purchased CEA protein and Anti-CEA antibody from abCAM and polydimethylsiloxane (PDMS) elastomer and curing agent from Coring, respectively. Nano pure deionized (DI) water ( $18.1\text{ M}\Omega\text{-cm}$ ) was produced in-house.

**Multilayer MoS<sub>2</sub> fabrication:** We used a micro-printing method to fabricate a multilayer-MoS<sub>2</sub> photoconductive nanosheet channel on a SiO<sub>2</sub>/Si substrate.<sup>[1-5]</sup> The printed MoS<sub>2</sub> nanosheet channel had a thickness of  $\sim 14.5\text{ nm}$ , showing a sufficient photoresponsivity at  $\lambda = \sim 650\text{ nm}$ . A Ti (5 nm) - Au (50 nm) electrode pair providing as the drain and source contacts for the MoS<sub>2</sub> channel was subsequently fabricated using photolithography, which was followed by metal deposition and lift-off. The resulting channel length and width were  $\sim 5$  and  $\sim 10\text{ }\mu\text{m}$ , respectively. We characterized the topography of the MoS<sub>2</sub> nanosheet channel using an atomic force microscope (Bruker ICON AFM). Tapping mode scan (scanning speed:  $0.1\text{ }\mu\text{m}/\text{sec}$ ) was performed using an AFM tip with the cantilever resistivity ranging from  $0.010$  to  $0.025\text{ }\Omega\text{ cm}$  in antimony n-doped silicon. We post-processed the obtained topographical data using commercial software (Nanoscope Analysis). The fabrication of photodetectors made of these MoS<sub>2</sub> channels followed the same lithographical patterning and etching processes in Figure S2.

**Noise Characterization of MoS<sub>2</sub>:** Assuming the shot noise of photodetectors as the main noise source, the measured noise current  $i_N$  is defined as  $i_N = (2e * I_{dark})^{1/2}$ , where  $e$  is the electric charge and  $I_{dark}$  is the dark current. We obtained noise power spectral density ( $i_N^2/\text{Hz}$ ) curves for a commercial CdS (Cadmium Sulfide) photodetector, a MoS<sub>2</sub> channel, and the analyzer

system, respectively. Every measurement for the photodetectors was performed under the dark condition at  $V_{DS} = 0.2$  V with no gate bias applied. The lowest measurable noise level of the system was confirmed by repeating measurements with suspended probe tips. The noise spectral density curve of the system shows a flat spectral noise density (i.e., a clear  $1/f$ -noise component), which indicates the noise floor of the measurement system. We performed all measurements using a semiconductor analyzer (Keithley 4200A).

**Gold nanoparticle functionalization with antibody:** At first, we centrifuged a solution suspending gold nanospherical particles (AuNPs) (0.2 nM) three times at 5,000 rpm for 10 min and washed the AuNPs in D.I. water to remove excessive structure direction agents (citrate) from the solution. Subsequently, we functionalized the AuNPs with thiolated alkane 10-Carboxy-1-decanethiol (HS-(CH<sub>2</sub>)<sub>10</sub>-COOH) using a self-assembly method (SAM). In this process, AuNP colloidal solution was first incubated in 1mM of thiolated alkane 10-Carboxy-1-decanethiol (HS-(CH<sub>2</sub>)<sub>10</sub>-COOH) overnight. Then, the antibody was linked to the -COOH functional group formed on the AuNP surface by means of standard 1-ethyl-3-[3-dimethylaminopropyl] carbodiimide / N-hydroxysuccinimide (EDC / NHS) coupling chemistry. Here, we first washed the -COOH functionalized AuNPs and loaded these AuNPs into a mixture of 0.4 M EDC and 0.1 M NHS at a 1:1 volume ratio in a 0.1 M EDC solution to activate the AuNP surface. We loaded a solution of primary CEA antibodies diluted from 100 to 10  $\mu\text{g}/\text{mL}$  in 1x PBS into the micro-tube holding the solution of the AuNPs functionalized above and incubated it for 60 min. To suppress fouling of the AuNP surface due to non-specific binding, we treated the prepared antibody-AuNP conjugates with 1% BSA in 1x PBS in blocking buffer and incubated the whole system for 20 min. Before the assay measurement of CEA, the antibody-AuNP particles were thoroughly washed three times to remove any excessive solutions or molecules using 20 $\mu\text{L}$  of 1xPBS. In addition, we obtained the extinction spectrum of the AuNP colloidal solution before and after the functionalization using a UV-VIS

spectrometer (Agilent 8453 G1103A Spectrophotometer) to confirm the AuNP functionalization.

**Assembly of multilayer MoS<sub>2</sub> channel-integrated colorimetric reader device:** We prepared a micro-chamber on a thin SiO<sub>2</sub> layer (Thickness = 250 μm) and the multilayer-MoS<sub>2</sub> channel on a silicon substrate, individually. We attached a medical grade double-sided tape (3M, thickness = 100 μm) onto the drain and source electrodes of the multilayer-MoS<sub>2</sub> channel. Next, we assembled them by placing the micro-chamber on the multilayer-MoS<sub>2</sub> channel along the marks under a stereo microscope (Olympus SZ61 Stereo Microscope) with a gentle press to ensure the attachment. After the assembly, we inspected the alignment using an optical microscope (Olympus SZ61 Stereo Microscope) and ensured the attachment between the micro-chamber and the multilayer-MoS<sub>2</sub> photodetector by flipping the assembled structure.

**Experimental setup for the assay:** In our homogenous plasmonic colorimetric assay, we mixed a biofluid sample with the plasmonic probe, loaded the mixture into the micro-chamber of the device, and measured photo current using an HP-4145B semiconductor parameter analyzer. Here, we used a 650 nm laser (power density, 2.5 mW/cm<sup>2</sup>) to characterize the photo response performance of the devices. For the control study, we also used a 532 nm laser power density (2.5 mW/cm<sup>2</sup>). We also measured the power density using a conventional power and wavelength meter (OMM-6810B-100V, Newport). The power density was tuned by neutralized density filter.

**Gold standard ELISA:** A 96-well plate of CEA ELISA kit was developed in our laboratory as described previously.<sup>[6]</sup> Briefly, each well of a 96-well plate was coated with 0.2 μg of anti-CEA antibody (capture antibody) and incubated overnight at 4°C, then it was blocked with a blocking buffer (Thermo Scientific, Rockford, IL, USA) at room temperature (RT) for 2 h. We

loaded sample solution onto the prepared plate. After 4 times of washing, anti-CEA antibody (1:3000 diluted) was added as detecting antibody and incubated at room temperature for 2 h. Following 4 times of washing, anti-peroxidase-labeled secondary antibody (1:50000 diluted) was incubated in the wells at room temperature for 1 h. After removing extra secondary antibodies with 4 times of thorough washing, the plate was developed with 3, 3', 5, 5'-Tetramethylbenzidine (TMB) for 20 minutes in dark, followed by dispensing a stop solution. CEA levels were determined using a plate reader at  $\lambda = 450$  nm.

**Electromagnetic field simulation:** We conducted a finite element analysis (FEA, COMSOL Multiphysics software) to predict the near-field electromagnetic fields around a dispersed AuNP and assembled AuNPs by solving Helmholtz wave equation. We constructed hybrid mesh structures for the AuNPs and their interparticle nanogap to fit their round shapes. In this analysis, we assumed that the relative permeability and complex permittivity of gold were 1 and  $\varepsilon_r = f(\lambda)$ , respectively. In addition, the model assumed perfect absorption at the outer boundary to minimize spurious reflections by setting a perfectly matched layer and an integration layer in a concentric space. According the SEM images in Figure 3, we defined the represented dimensions of the AuNP and the nanogap to be  $d = 50$  nm and  $g = 1$  nm, respectively. The simulation shows that the surface plasmon of the AuNP is strongly excited at  $\lambda = 532$  nm and  $\lambda = 650$  nm.

**Human whole-blood and serum samples:** Human blood samples were drawn from a healthy donor after obtaining informed consent according to an Institutional Review Board (IRB)-approved protocol (protocol HUM00115179/UMCC 2016.051). Some of specimens were collected and aliquoted in ethylenediaminetetraacetic acid tubes, and processed to obtain plasma and serum within 3 h.

**Standard artificial saliva and urine:** We used artificial saliva by dissolving 5 mM of NaCl, 1 mM of CaCl<sub>2</sub>, 15 mM of KCl, 1 mM of citric acid, 1.1 mM of KSCN, and 4 mM of NH<sub>4</sub>Cl in distilled water. The pH of artificial saliva was adjusted to 6.7, which is the average pH of healthy human saliva<sup>49-51</sup>. We also purchased artificial urine from Carolina Biological Supply Company (Burlington, NC).

**Table S1. Detection performances of commercialized human CEA ELISA kits.**

Commercialized human CEA ELISA kits	LOD	Time to results	Volume
Invitrogen	200 pg/mL	4 hr 45min	100 $\mu$ L
Boster	20 pg/mL	8 hr	100 $\mu$ L
Sigma-Aldrich	200 pg/mL	5 hr	100 $\mu$ L
Abcam	200 pg/mL	5 hr	100 $\mu$ L
Raybiotech	200 pg/mL	5 hr	100 $\mu$ L



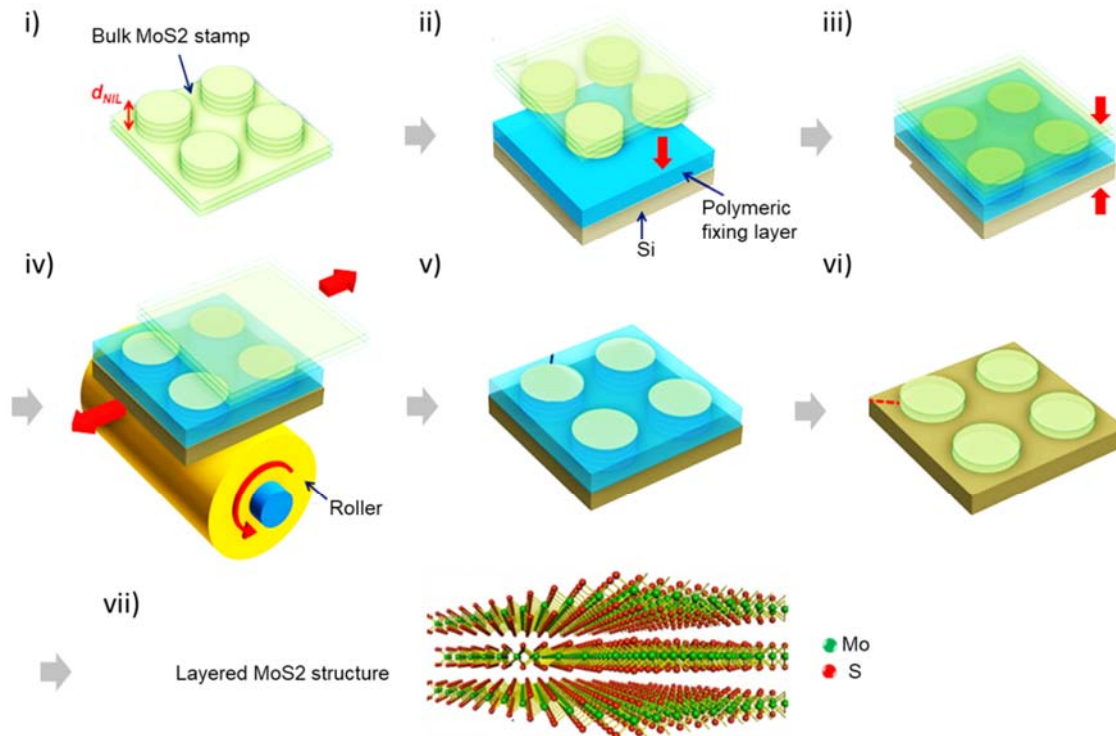


**Figure S1. Micro-printing-based MoS<sub>2</sub> pattern fabrication.** i) Preparing a bulk MoS<sub>2</sub> stamp, ii) Transferring the bulk stamp onto a Si substrate coated with a polymeric fixing layer, iii) Performing nanoimprint to push the bulk stamp against the polymeric fixing layer, iv) Applying shear exfoliation, v) Forming exfoliated MoS<sub>2</sub> patterns, vi) Removing the polymeric fixing layer, vii) Illustration of the layered structure of the fabricated MoS<sub>2</sub> pattern.

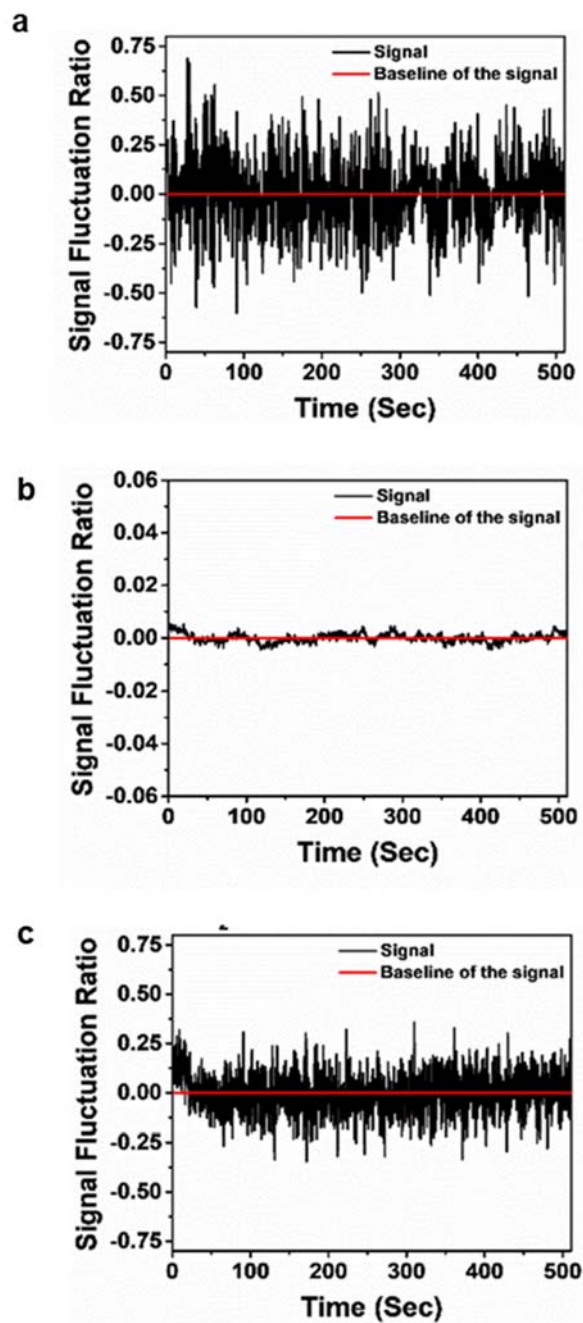


**Figure S2. Time-domain root-mean-square (RMS) noise values of MoS<sub>2</sub> photoconducting channels.** Representative data of (a) Pristine 3 nm-thick MoS<sub>2</sub> channel, (b) Pristine 14 nm-thickness MoS<sub>2</sub> channel, and (c) O<sub>2</sub> plasma treated 14 nm-thick MoS<sub>2</sub> channel.

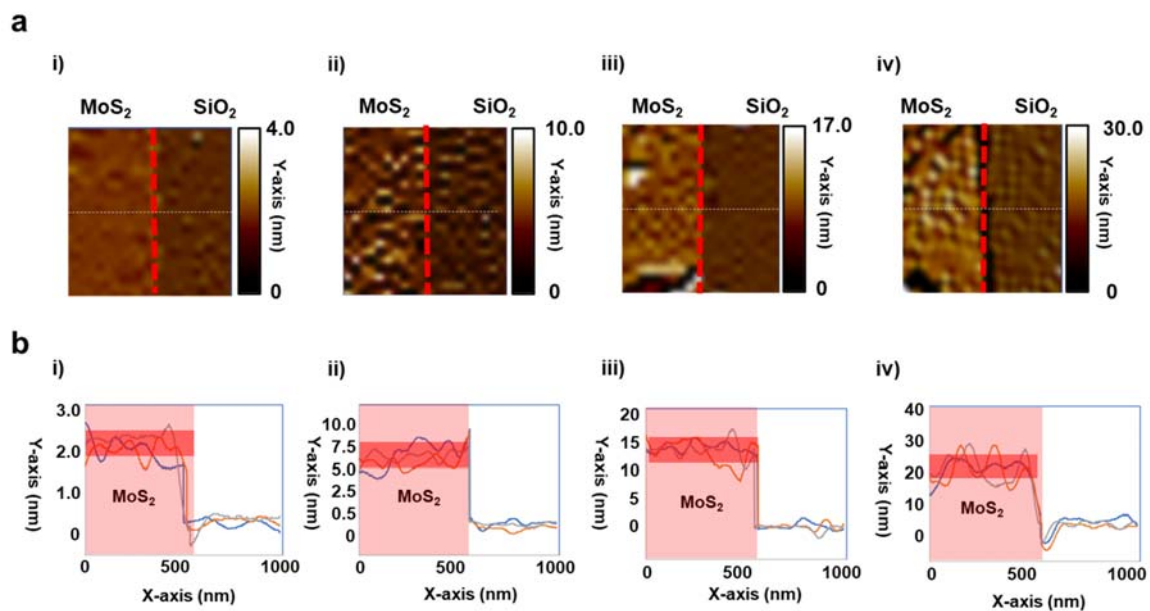


**Figure S3. AFM (a) images and (b) thickness profiles of MoS<sub>2</sub> layers i) 2.5, ii) 7.5, iii) 12.5, and 25 nm.**

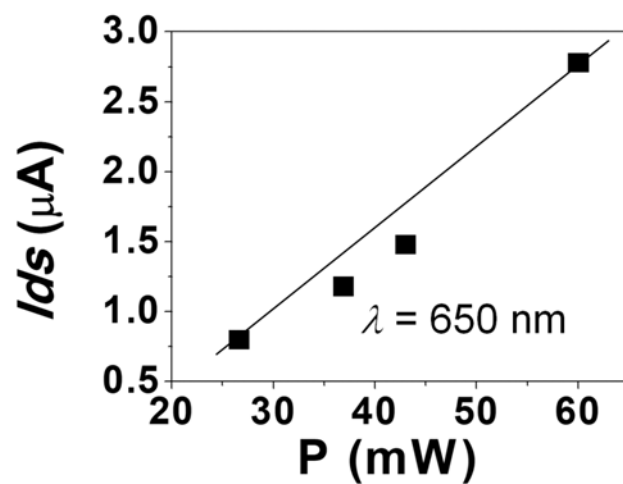


**Figure S4. Multilayer MoS<sub>2</sub> channel photocurrent as a function of illumination power.** The photocurrent between the source and drain of the channel at the source-drain voltage of 1V increases almost linearly with the incident light power ranging from 25 to 60 mW.

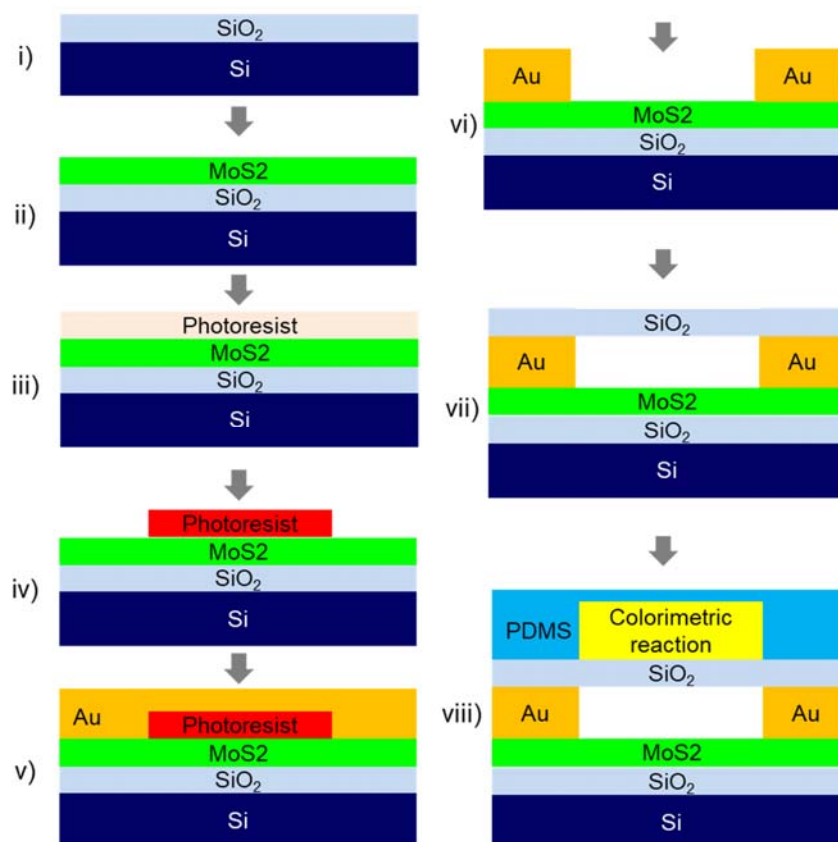


**Figure S5. Fabrication steps of multilayer MoS<sub>2</sub> channel-integrated colorimetric reader device.** i) Thermally growing a SiO<sub>2</sub> layer on Si substrate, ii) Synthesizing a large-area (2 cm × 3cm) MoS<sub>2</sub> blanket layer onto the SiO<sub>2</sub>/Si substrate by chemical vapor deposition (CVD). iii) Spin-coating photoresist (SPR 220) at 4,000 rpm and soft-bake the substrate at 115 °C for 1 min to remove the solvent. Patterning the photoresist layer by UV light exposure using a mask aligner (MA6, Karl Suss) and develop it. Then, loading the substrate into a plasma etching chamber (Xactix XeF<sub>2</sub>), etching the exposed MoS<sub>2</sub> with 2 Torr XeF<sub>2</sub> for 10 second, and stripping off the photoresist to form the MoS<sub>2</sub> channel pattern. iv) Depositing and patterning the second photoresist layer. v) Depositing a Ti (5 nm)/Au layer (50 nm) on the patterned second photoresist layer using an electron beam (e-beam) evaporation system (Enerjet Evaporator). vi) Lifting off the photoresist to pattern a pair of electrodes that provide drain and source contacts for the MoS<sub>2</sub> channel (length: 1 μm, width: 10 μm). vii) Placing a SiO<sub>2</sub> substrate (t =100 μm) on top of the banks of the Au electrodes. viii) attaching a soft lithographically molded PDMS layer whose surface is treated by O<sub>2</sub> plasma at P = 18 W for 2 min to the SiO<sub>2</sub> substrate. The assembly of the micro-well originally created in the PDMS layer and the SiO<sub>2</sub> substrate forms the colorimetric reaction micro-chamber.

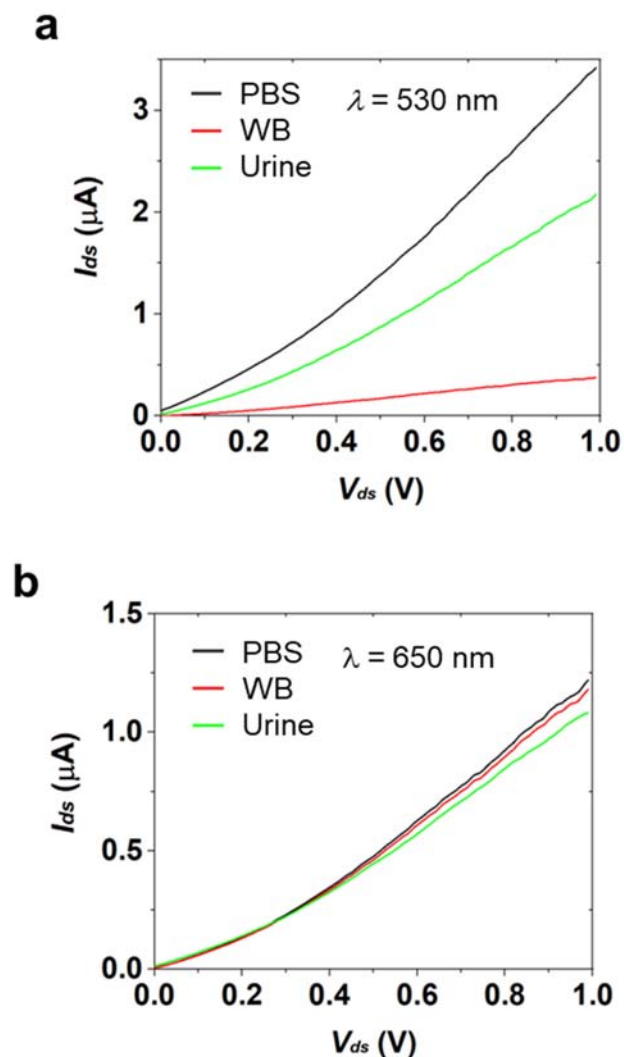


**Figure S6.  $I$ - $V$  curves of multilayer  $\text{MoS}_2$  channel-integrated colorimetric reader device loaded with PBS, WB, and Urine with excitation illumination at (a)  $\lambda = 530 \text{ nm}$  and (b)  $\lambda = 650 \text{ nm}$ .** The photocurrent of the  $\text{MoS}_2$  photodetector channel  $I_{ph}$  was measured while sweeping the source-drain voltage from 0 to +1 V for PBS, WB, and Urine samples unmixed with the antibody-AuNP solution and loaded to the micro-chamber of the reader device. The used illumination power was  $P = 2.5 \text{ mW}$  for both (a) and (b). The smaller  $I_{ph}$  values at  $\lambda = 530 \text{ nm}$  for WB and Urine are due to light absorption in those biofluids. In contrast, the  $I$ - $V$  curves show small differences between PBS, WB, and Urine at  $\lambda = 650 \text{ nm}$ , which implies small light absorption in WB and Urine in the NIR region.

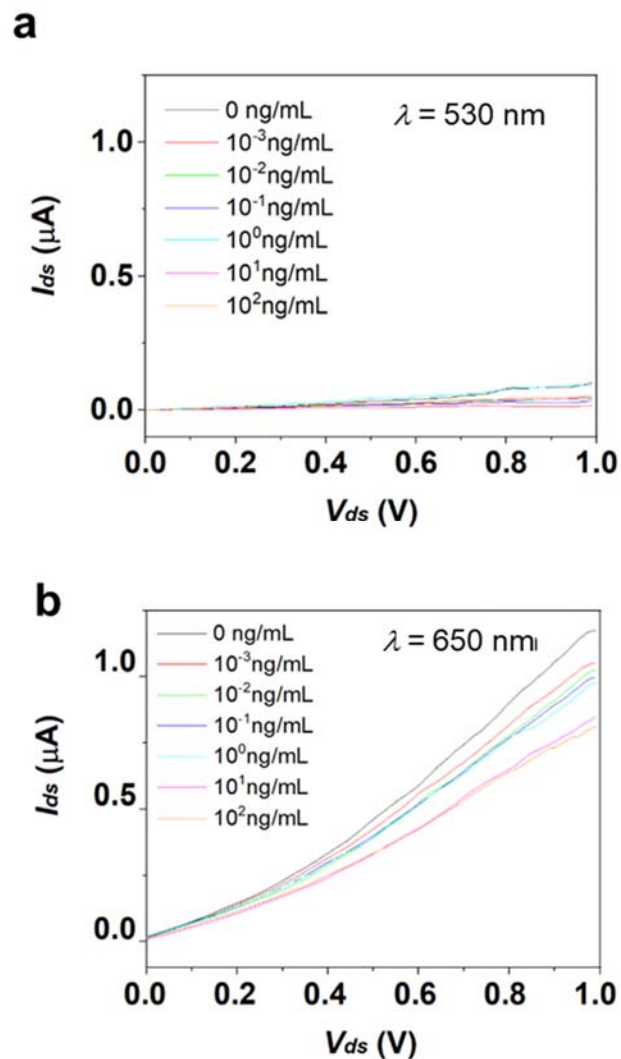


**Figure S7. I-V curves of multilayer MoS<sub>2</sub> channel-integrated colorimetric reader device for various CEA concentrations with excitation illumination (a)  $\lambda = 530 \text{ nm}$  and (b)  $\lambda = 650 \text{ nm}$ . These I-V curves were used for calibration of the plasmonic colorimetric biosensing assay of CEA in WB. The used excitation illumination power was  $P = 2.5 \text{ mW}$  for both (a) and (b). As expected from the data in Fig. S6, the curves at  $\lambda = 530 \text{ nm}$  show the weak photoresponse of the device due to light absorption in WB.**

**References**

- [1] M. Chen, H. Nam, H. Rokni, S. Wi, J. S. Yoon, P. Chen, K. Kurabayashi, W. Lu, X. Liang, *ACS Nano* 2015, 9, 8773.
- [2] M. Chen, H. Nam, S. Wi, L. Ji, X. Ren, L. Bian, S. Lu, X. Liang, *Applied Physics Letters* 2013, 103, 142110.
- [3] M. Chen, H. Rokni, W. Lu, X. Liang, *Microsystems & Nanoengineering* 2017, 3, 17053.
- [4] H. Nam, S. Wi, H. Rokni, M. Chen, G. Priessnitz, W. Lu, X. Liang, *ACS nano* 2013, 7, 5870.
- [5] S. Wi, H. Kim, M. Chen, H. Nam, L. J. Guo, E. Meyhofer, X. Liang, *ACS Nano* 2014, 8, 5270.
- [6] Y. Park, B. Ryu, Q. Deng, B. Pan, Y. Song, Y. Tian, H. B. Alam, Y. Li, X. Liang, K. Kurabayashi, *Small* 2020, 16, 1905611.